Conf-9204105--1

RESULTS OF MACE TESTS M0 AND M1

B. W. Spencer[1], M. T. Farmer[1], D. R. Armstrong[1], D. J. Kilsdonk[1], R. W. Aeschlimann[1], and M. Fischer[2]

[1]Argonne National Laboratory
Argonne, IL 60439 USA

[2]Siemens AG
UB KWU FRG

ANL/CP--75574

DE92 010348

ABSTRACT

The Melt Attack and Coolability Experiment (MACE) Program underway at Argonne National Laboratory under ACE/EPRI sponsorship is addressing the efficacy of water to terminate an accident situation if melt progression were to result in a molten core/concrete interaction (MCCI) in the reactor containment. Large-scale experiments are being conducted in parallel with related modeling efforts, involving the addition of water to an MCCI already underway. The experiments utilize $UO_2/ZrO_2/Zr$ corium mixtures, direct electrical heating for simulation of decay heating, and various types of concrete basemats. Currently the tests involve 430 kg corium mass, 25 cm depth, in a 50 cm square test section. Test M0 was a successful scoping test, but the first full size test, M1, failed to achieve melt-water contact owing to existence of a preexisting bridge crust of corium charge. A heat flux of 3.5 MW/m^2 was measured in M0 which removed energy from the corium pool equivalent to its entire heat of solidification prior to abatement by formation of an interfacial crust. The crust subsequently limited heat extraction to 600 kW/m^2 and less. Both tests M0 and M1 revealed physical evidence of large pool swelling events which resulted in extrusion (and ejection) of melt into water above the crust, significantly increasing the overall quench and reducing the remaining melt in contact with the concrete. Furthermore, test M1 provided evidence of occasional "burst mode" ablation events and one additional important benefit of overlying water--aerosol capture.

MASTER

INTRODUCTION

Research programs are currently underway which address the question "What about the use of cavity flooding operations if a core melt accident were to progress to the 'core-on-the-floor-scenario' such that a vigorous molten core-concrete interaction (MCCI) were underway." An MCCI, if unabated, raises serious concerns about the possibility of basemat erosion or even meltthru, heat addition to the containment atmosphere, weakening of important containment structures, release of noncondensable, combustible gasses to the containment atmosphere, and release of copious amounts of aerosol including radioactive matter to the containment atmosphere. Programs are currently underway addressing the possible role of water to abate the above processes with the goal of eventually terminating and stabilizing the MCCI. These programs are WETCOR at Sandia National Laboratories, sponsored by the USNRC, and the Melt Attack and Coolability Experiments (MACE) underway at Argonne National Laboratory under sponsorship of the international Advanced Containment Experiments (ACE) Consortium. The ACE/MCCI and ACE/MACE programs are described by Sehgal et. al. in Refs. 1 and 2. This paper describes the initial phases of development of the MACE experiment program with emphasis on findings from early MACE tests.

OBJECTIVES/APPROACH

The general objective of the MACE program is to explore the possible benefits of massive addition of water to an MCCI already in progress insofar as:

- energy extraction and stabilization of the heat generating core debris,
- arrest or even terminate basemat ablation,
- reduce thermal load to key structures,
- scrub released aerosols.

The approach used in the MACE tests is to utilize selected PWR or BWR core melt compositions comprising UO_2, ZrO_2, Zr and possible control rod materials. Direct electrical heating (DCH) is used to produce bulk internal heat generation, and the power level is controlled to nominally depict the volumetric decay heat power level for the particular reactor type at some length of time into the accident. The ACE and MACE tests have typically used full decay heat at 2 hrs (i.e., ~350 watts/kg UO_2 for a PWR); heretofore, no account has been taken for reduction in this heating owing to release of volatiles from the fuel in the reactor accident. The DEH heating method takes advantage of the semiconductor-type property of UO_2.

Hence the ACE and MACE tests are best suited for core melt compositions wherein the oxide is the dominant phase. This is potentially complementary to KfK BETA and SNL WETCORE and SURC facilities where induction heating methods favors, but is not exclusive to, mainly metal compositions. The DEH heating method can be computer controlled to operate at constant power, current, or voltage, depending on the specific application. In general, the method shows sensitivity to:

- melt temperature (resistivity decreases as temperature increases),
- melt composition (generally increased resistivity with increased dilution of UO_2),
- flow area (resistance increases as flow area decreases).

These sensitivities were not a problem for the ACE/MCCI tests where a constant power mode of operation was used. The power supply voltage typically increased to accommodate the dilution effect of concrete decomposition products CaO and SiO_2 entering the melt. However, the MACE tests are proving to be more challenging since not only does the composition change if long term basemat erosion occurs, but there are also short term effects of quench-related temperature drop and also changes to flow area as will be described later. Hence an important current MACE task is to improve our ability to interpret test results by development of a comprehensive DEH model taking into account sensitivities to all parameters. When this is completed, somewhat more quantitative DEH-related results may be available than at present.

MACE EXPERIMENT DESCRIPTION

The major elements of the MACE apparatus are shown in Fig. 1. The apparatus consists of a test section about 3 m tall. At the bottom of the test section is the concrete basemat, instrumented with Type K TC-s to measure downward heatup and erosion rate and W-Rh TC's in tungsten thermowells to measure MCCI-zone temperatures. The corium charge is placed atop the concrete. This charge is in the form of crushed UO_2 pellets (unirradiated, natural or depleted) plus particles of ZrO_2 and typically a small amount of concrete decomposition product oxides CaO, SiO_2. Their presence is to create a lower, more prototypic melting temperature than a pure UO_2, ZrO_2 system, and furthermore can be rationalized from consideration of the reactor case involving a small amount of erosion that can occur when the melt flows from the breached vessel onto the basemat floor [3]. A region of UO_2 crushed pellets is initially heated by tungsten heater elements until its temperature is such that oxide phase conductance begins. The zone experiences first localized melting, and the melted zone grows to encompass eventually nearly all the loaded powders as the DEH power is gradually increased accordingly.

Different techniques have been used to add Zr to the molten oxide system. The most successful technique, employed in these tests, has been to use Zr rods, 12.7 mm dia placed crosswise to the direction of current flow at the interface between the charge and the basemat proper. The Zr is melted and concurrently mixed with the overlying oxide-phase melt by action of the concrete decomposition gasses. Some of the Zr is necessarily oxidized during this ingression phase, limited by the offgassing during this stage. The MCCI proper is defined to begin after ablation through the Zr-bearing zone is completed, typically defined by a zero-reference elevation thermocouple. The metallic Zr in the melt at this starting time is reduced according to the amount of prior oxidation.

The MACE apparatus differs significantly from the ACE/MCCI apparatus [1] in that the latter utilized a water-cooled test section to facilitate measurement of directional heat transfer as well as enable quasi-steady long term tests. The MACE apparatus is not cooled except for the water to be added during the MCCI; otherwise it depends upon the heat capacity of the vessel structure. Argon gas is bled into the test section to cool the concrete decomposition gas and aerosols released prior to water addition.

At a specified depth of concrete erosion, following addition of Zr, the water addition is initiated. A water supply/delivery system is provided for this purpose. Water at room temperature is metered at selectable flowrate into the test section. It is delivered by two wiers at the top of the test section in the walls adjacent to those having the electrodes. Initially, water is added steadily until a 50 cm head is established above the melt layer as recorded by redundant head measuring devices in the test section. Thereafter, the water is added intermittently to maintain a 50^{+5}_{-10} cm level as boiloff progresses. Thermocouples in the test section measure the water and cover gas region temperatures. The vertical dimension of the test section was sized such that roughly the upper one meter would be available for water droplet settling even if the corium and water pools were churn-turbulent owing to the vigorousness of gas sparging.

A large gas line is present in the top cover to duct dilution gas, noncondensable offgas, and steam to the adjacent quench tank. The quench tank provides a mass of water to condense transported steam and to cool other gases. Condensate spills over and is collected in the overflow tank. The quench tank has a cooling coil to maintain its water inventory in a subcooled state. The cooling coil, quench tank, and overflow tank are instrumented with flowmeters, thermocouples, level sensors, and pressure transducers in order to monitor the transient state of the system and extract the necessary heat balance information. Downstream from the quench tank is a spray tank which performs a redundant quench/gas cooldown function. While adding redundancy, the use of two quench tanks in series is designed to enhance resolution of the energy transport measurement. This overcomes the practical difficulty of attempting to make energy transport measurements equivalent to melt-to-water heat fluxes ranging from as high as 5 MW/m^2 during a postulated early bulk cooldown stage to as low as a few hundred or less kW/m^2 depending upon possible crust behavior. Both low and high energy transport rates can be reliably measured with the approach described here.

The Argon dilution gas and noncondensable offgas species (CO_2, CO, H_2) are cooled to near room temperature by transport through the quench tank water and spray tank water, and exit the system through an exhaust line at the top of the spray tank. The line includes a demister, filter, gas flowmeters, and a gas mass spectrometer to give the time-varying composition of the gas. This gas is released directly into the exhaust line of the containment cell ventilation system where it passes, further diluted, through a final cleanup system before being released via the building stack. The entire MACE apparatus is housed within a containment building formerly used for a (dismantled) research reactor at ANL. This containment building provides convenient radiological control measures as well as protection from postulated end-of-spectrum steam explosion and hydrogen behavior effects.

Greater detail on equipment, instrumentation, data acquisition, and procedures is available in Project documentation.

MACE SCOPING TEST (M0)

The MACE scoping test was conducted for two principal purposes: 1) to get an early indication of the mode and extent of corium quenching as an aid to both model development and future experimentation, and 2) to demonstrate that the DEH internal heating method would work with water atop the corium melt. As regards the latter, analysis had indicated that no more than, and probably far less than, 1% of the DEH energy generation would occur in the water via the water parallel electrical path. Formerly this was controversial, but subsequent test results have revealed no anomalies attributable to water parallel path.

The M0 test was performed using equipment available from the ACE/MCCI program. It utilized ACE technology and experiment team while maintaining a parallel ACE/MCCI schedule. The scale was selected to be 30 cm x 30 cm test section with a corium mass of ~130 kg, equivalent to ~15 cm collapse pool depth. This size and mass reflected an upper operational limit of the available 300 kW power supply (not from the power standpoint, but from the available voltage/current ranges). The size was slightly larger than the 21.6 cm dia vessel used in previous SWISS tests at SNL in which water was added atop molten stainless steel interacting with concrete in a MgO crucible [4]. In both those tests an upper bridge crust formed at the melt-water interface which prevented any significant abatement of the melt-concrete interaction. For the MACE M0 test it was decided to use concrete not only for the basemat but also for the sidewalls. The rationale was that any crust material formed in M0 would be unlikely to anchor to the sidewall if the sidewall were a readily decomposing material. This decision addressed the heart of the concern about quench tests performed at small scale, but, regrettably, this approach did not prevent crust anchoring as will be described.

Conditions for the M0 test are listed in Table 1. These conditions were closely patterned after the ACE L1 test involving PWR corium composition with about 30% of the zirconium in unoxidized, metallic form, interacting with a limestone/common sand concrete basemat. The heat generation was specified to be 350 watts/kg UO_2 (26 kW total to the corium). However, the test was actually run at a power from 2x to 4x the specified power because the melt was at such low temperature compared to the operator's L1 experience, as will be described.

The M0 test was conducted August 24, 1989. Water addition was planned to begin when the basemat centerline thermocouple array indicated ablation had proceeded 1.2 cm below the elevation of the Zr rods. When this depth was attained, it was evident in the video that the melt pool was highly agitated and that there was no significant floating crust on the pool, but also that there was a partial crust (remnants of the original powders) which had not collapsed into the pool. This crust appeared to be cantilevered from the electrodes and extended outward about one-quarter of the test section width in the visible quadrant. Although not visible in the video, this cantilevered partial crust probably existed along the opposite electrode side as well. If so, it is estimated that the test section area was about one-half occluded by the sintered powders, albeit the surface of the melt itself was probably several centimeters below the elevation of this partial crust. Other test data revealed that the melt was attacking the basemat in an asymmetric profile; it had started in the southwest quadrant, proceeded to the central quadrant, and would later progress to the northeast quadrant. The experimenters did not observe the extremely intense interaction which accompanied the Zr ingression stage of the MCCI L1 test, and so left the power at the heatup level of about 100 kW rather than reduce it to 26 kW as planned.

Water was added to the test section at an initial rate of 10 l/s until the desired pool depth of 50 cm was attained. Makeup flow was added to maintain this level during boiloff. Figure 2 shows the cumulative energy transported from the test section to the quench tank via the steam and gas flow. This data has been corrected for heat transfer from apparatus structures other than heat flux from the melt pool itself. The data indicates that during the first three minutes of contact, there was an intense extraction of heat from the melt amounting to 3.5 MW/m^2, related to the planar cross-sectional area of 0.090 m^2. The energy extracted from the corium during this initial contact stage amounted to 44 MJ. Using a heat of fusion for the corium melt of about 0.3 MJ/kg and a corium mass of 130 kg, it can be seen that the measured energy extraction could have largely, if not completely, solidified the corium mass, albeit leaving it at very high temperature. Even if uniform bulk cooling were not achieved in an ideal sense during this early interaction stage, it is clear that a significant cooling transient occurred which would have resulted in slurry formation and thereby increased melt viscosity. Regrettably, the thermocouples in MO did not capture this event owing to the asymmetric corium attack on the basemat.

While the fist three minutes of contact were characterized by intense energy extraction, this stage was immediately and rather suddenly followed by a quite quiescent period for the next three minutes. The most plausible explanation for this has been put forth by Farmer et. al. [5] who relate the stability of an interfacial crust to the gas sparging rate attributable to the concrete decomposition. That is, the large energy extraction during the initial interaction period so stabilized the corium that basemat attack, and thereby gas sparging rate, were greatly reduced. The Farmer model would predict a stable interfacial crust to form under such conditions. Indeed, we know from posttest examination that a bridge crust did form in this scoping test, and it is suggested that this first happened during the quiescent period from 3-6 min after water addition.

There is further indication of this from interpretation of the ablation data. Figure 3 shows basemat ablation as indicated by the centerline array of TC's attaining the concrete liquidus temperature of 1568 K [6]. The TC junctions are at discrete depths into the concrete; the straight line segments drawn through the actual data in Fig. 3 reflects the author's interpretation of a plausible trend. The initial ablation rate was 2.3 mm/min as recorded up to the time of water addition. After water addition (at 4.0 min) the ablation rate measures ~1.8 mm/min, but with an offset equivalent to ~6 min. It is interpreted that the cooling transient could in fact have stabilized the MCCI during this time, but with continued internal heat generation (~4x decay heat at this time during MO), a reheating occurred and the MCCI resumed.

It is important to note that in this small scale experiment, the bridge crust was well anchored by the tungsten electrode rods. The crust remained at the elevation where it formed as the resumed MCCI caused continued downward erosion of the melt into the concrete. At reactor scale, analyses suggest that the crust would break up and remain in contact with the melt [7]. Moreover, it is worthwhile to note in this test that the crust was also firmly attached to the concrete sidewalls. The use of an ablative wall material as an attempt to preclude that attachment was not successful owing to the cooling effect of the overlying water at the boundary.

The quench data in Fig. 2 shows that following the quiescent period the energy extraction from the melt pool resumed. While several perturbations are present, the general trend shows 600 kW/m^2 up to ~35 min and then a gradual diminishing to as low as 150 kW/m^2 by the end of the test. For comparison, the upward heat extraction to remove all the decay heat in a 15 cm deep corium pool is ~290 kW/m^2. The MO test was run with diminishing power which was ~4x decay heat early in the test and reduced to ~2x by the end of the test. Hence early in the test at the 600 kW/m^2 upward heat extraction rate the upward downward heat transfer was about 50/50; by the end of the test it had reduced to about 30/70. The crust thickness may be estimated from

$$\delta = \frac{k \Delta T_c}{q''}$$

where $k \simeq 1 \frac{W}{m \cdot K}$ and ΔT_c = temperature drop across the crust ≃2100 K based on the underside temperature equal to the corium liquidus of ~2500 K and the top surface at T_{sat} = 373 K (nucleate boiling). This thickness is ~4 mm at the 600 kW/m^2 flux, and increases to an equivalent thickness of ~14 mm by the end of the test. The actual crust which was examined after the test (Fig. 4) was ~2 cm thickness in the central region and up to ~5 cm thickness where it was anchored to the electrodes.

Nature displayed a very remarkable phenomenon in this test which has also been observed in later WETCOR and M1 tests. Periodically, there was ejection of molten corium through the bridge crust into the overlying water. In MO these ejections were driven by release of MCCI decomposition gas such that melt entered the water in a dispersed droplet mode. These droplets were quenched duri[illegible] their flight through the overlying water. They fell back onto the bridge crust and formed a deepening, quenched particle bed atop the crust (Fig. 4). Be the end of the test this ejected debris had formed a bed about 10 cm in depth of which the top half was loosely packed particles and the lower half was rather hard sintered agglomerate approaching the character of the fully dense crust itself. The masses of debris in these two zones amounted to 10.1 and 12.5 kg, respectively. Hence, a corium mass amounting to nearly 20% of the original amount became fully quenched and coolable by a dispersive mechanism completely separate from the quasi-steady conduction limited heat transfer through the crust.

The times of the discrete eruptions are shown in relation to the quench data in Fig. 2. The events numbered 1 through 5 were visible in the test section video during the test as well as afterwards. Events 3 and 4 caused a jump in the quench data amounting to about 22 MJ each. Other events had considerably smaller effects on the quench rate. Events 1b and 1c are not visible on the video but are known to have occurred from correlation with other test data. The power supply current was sensitive to these events, showing a sharp decrease at the onset of each dispersal; this is interpreted as a loss of conductor (melt) from the electrical path, although other factors may also have played a role. The melt pool temperature appeared to decrease at Events 2, 3, and 4, although this interpretation is not completely consistent for all events.

Each of the dispersive events 1b through 4 correlates perfectly with peaks in the measured gas flowrate data. The gas mass spectrometer was not used for M0 owing to its installation in the ACE/MCCI facility. Hence, only total flowrate data, and not breakdown by composition, was available for M0. The flowrate data indicated that up to t = 18 minutes, very little other than the argon bleed gas (82 slpm) passed through the system. There was no indication of the observed Event #1 at t = 15 min. However, events 1b through 4 are clearly evident as peaks in the flowrate curve at t = 20, 29, 38, 53, and 65 min. respectively. The flowmeter data shows that decomposition gas continually flowed through the crust from t = 18 min until termination at t = 84 min, with an exception that the crust appears to have been essentially plugged from Event 1c to Event 2. The data indicates large integrated gas releases attributable to Events 1b, 1c, and 2, but relatively little for Events 3 and 4, and essentially no spike-type release at all for Event 5. To understand the absence of a spike at Event 1 it must be postulated that essentially all the released noncondensable decomposition gas was in the form CO_2 (rather than H_2 and CO). Then a straightforward calculation reveals that the limit of solubility of CO_2 in the available water mass was not reached until about 18 min in the test as the data indicates. After that time the CO_2 passed through the system and was measured by the exit gas flowmeter.

The available quench water was exhausted in this test before the target ablation depth of 12 cm was attained. As a result, the test section experienced dryout at t = 75 min, but the corium internal heat generation was continued until t = 85 min. Hence, the final 10 minutes of the test was conducted without water atop the crust/debris layer. Event #5 occurred during this period at t = 81 min. The melt ejection took place through a volcanic-type vent hole in the central region of the test section and was visible in the quadrant viewed by the video camera. The camera captured visual evidence of melt droplets being blown through the vent hole as gas was being released. Although the gas release effects were visible, overall, this gas release was trivial compared to earlier events which coincided with large gas flowrate spikes; this event caused no detectable spike. Of particular interest was that the video also showed a single-phase extrusion of melt; the melt emerged from the hole, ran down the particle bed surface in the field of view, and froze in a manner reminiscent of a lava tube.

When the M0 test section was disassembled it was found that the concrete sidewalls had been eroded up to ~5 cm in the region of the original powders and as much as 10 cm in the MCCI zone below (Fig. 4). Thermocouple data indicated that sidewall concrete was being ablated into the corium charge as early t = -48 min and in some places had ablated to 1 cm depth at -35 min. It is estimated that at the onset of concrete ablation, the total corium mass amounted to ~130 kg of which 23% was concrete decomposition products and 4% was metallic Zr. The first available melt temperature data indicated ~2000 K, decreasing to ~1700 K by the end of the test. It is thought that the large influx of concrete from the sidewalls during the preheat stage depressed the melt temperature in this test to the extent that the zirconium (T_m = 2125 K) was not significantly melted. Unmelted rod segments were recovered after the test. Hence Zr oxidation would not have played an important role in this test which explains both the lack of expected agitation during Zr addition (based on L1 experience) as well as gas flowmeter behavior (since H_2 and CO which have very small solubility in water were not produced to any appreciable extent). Hence the actual M0 test conditions actually reflect a fully oxidized PWR corium composition ~30% diluted by concrete decomposition products run at ~2x to 4x prototypic decay heat power level.

Under these circumstances, was there anything of particular value in this scoping test? The answer is yes, not only from the standpoint of guiding future experiment efforts, but very notably from relevant information gained for model development. To recap, this test showed very large initial heat extraction from the melt pool which may, in fact, have stabilized the pool. Data suggests that basemat erosion may have been temporarily halted and that the bridge crust probably formed during this interval. Data showed the crust was porous to release of offgas, but there is no indication of water ingression into the MCCI zone through the crust in this small scale test. The crust firmly anchored itself to a decomposing sidewall material (concrete) owing to the quenching effect of the water. The test revealed for the first time a heretofore unobserved phenomenon which augmented the heat extraction from the corium; i.e., melt eruption through the crust and particle bed formation atop the crust. The test gave physical and visible evidence of large swelling of the corium pool into contact with the underside of the crust and associated extrusion of melt out the available passage. In general, however, the MCCI zone ablated away from the anchored crust, and the percentage of heat transferred upward through the crust diminished during the course of the test. At the end of the test the cavity between the underside of the crust and the collapsed melt surface measured 15 cm. The remaining melt pool was ~12 cm deep. Hence, the void fraction in the melt layer must have increased to 56% to cause contact with the crust and the observed single-phase melt extrusion through the crust passage. Examination of the underside of the crust indicated a smooth surface with a semi-regular wave contour of ~3 cm wavelength and 1-2 cm amplitude. This appearance suggested that the underside of the crust was melted at some time(s) during the test.

MACE TEST M1

Following the Scoping Test, the MACE facility was revised to allow larger scale tests of 50 x 50 and 75 x 75 cm size. The test section was constructed of MgO sidewalls rather than concrete to prevent the early concrete dilution of the corium and to avoid the undue suppression of melt temperature experienced in M0. The tungsten electrodes were recessed into the MgO walls. Instrumentation was considerably enhanced, including lance probes to detect the formation of a crust. For test M1 the test section size was 50 x 50 cm and the corium depth was 25 cm (collapsed pool depth); the corium mass was 430 kg. A mixture of Fe_2O_3 and Zr was blended with the corium charge in order that the chemical reaction would speed the corium preheat stage.

The M1 test was conducted November 25, 1991. Owing to three important defects, this test did not meet its objectives and is being rerun as M1b. However, the test provides some information which is worthy of note, and hence aspects of the test results are described here. The results reported here are of a preliminary nature since the focus of attention is now on successfully performing M1b.

First it is necessary to briefly summarize the shortcomings of M1. Test M1 was performed with a crust of original corium charge (sintered particles) spanning the top of the test section. This material never ingressed into the melting corium as experience in ACE/MCCI tests. The depth of powders above the igniter wires was somewhat greater in this test than usual practice. However, in retrospect the major contributing factor was the use of the exothermic chemical additives having a metallic reaction product which caused the preheat to progress inordinately rapidly in the downward direction in this test, leaving behind sintered but not melted charge materials along the walls and spanning entirely across the top of the test section. The operators knew of this from the lance probe detectors but could do nothing to rectify the situation. The decision was made to continue the test for its benefit as a facility shakedown test. Test M1 was not a test of melt-water interaction since the preexisting crust prevented melt-water contact from the onset and throughout the course of the test.

Continued operation of the test revealed two additional problems which diminished its usefulness as an L1 MCCI counterpart test. First, problems were experienced with one of the 100-channel MUX units. The unit was replaced with a spare but that also malfunctioned after only ~15 minutes operating time suggesting a more fundamental problem. Since this equipment was located inside the containment, no further troubleshooting could be undertaken. Hence the operators were deprived of essential readouts needed to track and control the experiment, and ~40% of the data was irretrievably lost. Lastly, it was found that the high-temperature thermocouples used in M1 performed very poorly, giving anomalous readings. Some of this data may be retrieved through testing of the TC's currently in progress.

In summary, the first difficulty described involving the initial overlying crust prevented M1 from achieving its melt-water interaction objectives. Loss of data from one of the 100-channel MUX's as well as anomalous behavior of the high temperature thermocouples prevented satisfactory diagnostics of the L1-type MCCI that did take place. These problems are being addressed for the M1b repeat of M1.

Despite the afore-mentioned difficulties, there is valuable information to be gleaned from M1. Test conditions are summarized in Table 1; conditions were very similar to the preceding M0 test except for the larger size. The conditions are also very analogous to the ACE L1 MCCI test performed at ANL April 25, 1989.

The M1 test ran for 3.0 hours from the onset of basemat ablation until the test was terminated at an ablation depth of 25 cm as indicated by the centerline thermocouple array. The preheat stage temperatures measured between 2200 and 2300 K. The test power ranged from 1x to 2x the desired heat generation rate. The overall average ablation rate was 1.4 mm/min. Figure 5 shows the individual data points which comprise the centerline ablation history. The data has a peculiar shape, but comparison with ACE test results indicates that the "burst-type" ablation pattern observed here, separated by relatively quiescent periods, is also evident in the details of the other ACE tests; the behavior depicted in Fig. 5 is not unique but is somewhat more pronounced here than observed previously.

It had been intended to add water to the test section when the ablation reached 2.5 cm. However, at that time the operators were preoccupied with instrumentation and crust-related issues. When the decision was made to proceed with water addition, it took place at t = 169 min when the ablation depth at the centerline was already ~10 cm. The average ablation depth over the entire basemat was ~8 cm. Figure 6 shows the measured heat flux data and integrated energy transport from the test section to the quench tank. The peak heat flux measured about 1.0 MW/m^2 when the water was first added to the test section, referenced to the test section area of 0.25 m^2. However, the heat flux from the corium would have been significantly less since this data has <u>not</u> been corrected for the transient quenching of the sidewalls and structures in the test section. This low heat flux, compared to the <u>corrected</u> values of 3.5 MW/m^2 measured in the scoping test, confirms that water merely contacted the bridge crust of sintered corium powders rather than the corium melt pool beneath it.

Consistent with the M0 results, there were melt eruption events which also occurred during this test. These events are shown in relation to the quench data in Fig. 6. Event 1 occurred at t = 161 min, prior to water addition. Periodic bursts of sparks were visible through the dense aerosol for about 30 seconds. Events 2 and 3 produced visible bursts of sparks in the overlying water lasting for 5 and 1 1/2 minutes at t = 229 and 270 min, respectively. According to other data, it is probable that unobserved extrusion events also occurred at t = 179 and 202 min, labeled Events 1b and 1c in Fig. 6.

The gas mass spectrometer indicated steady flow of noncondensable concrete decomposition gasses through the system. Prior to water addition the flowrate was ~200 slpm, about 95% H_2 + CO and 5% CO_2. By the end of the test this flow was ~120 slpm, about 80% CO_2 and 20% H_2+ CO. The data clearly shows the progressive oxidation of the metal constituent of the corium. With one exception there were no gas flowrate spikes attributable to the melt eruption events during M1. The preexisting crust of sintered charge material was sufficiently porous to the offgas flow that the melt eruptions could not be said to be blowdown events as was observed in M0. This data indicates that the eruption events cannot be attributed to gas pressurization in the cavity and subsequent breach of the crust. This is further indication of the inferred periodic volumetric swelling of the corium pool.

The exception alluded to above occurred at Event #1, prior to addition of water. At that time the offgas flowrate peaked at 700 slpm. Note in Fig. 5 that this time coincides with a burst of basemat ablation. According to other data, this occurred globally over a large part of the basemat area. It is interpreted that a burst of concrete erosion occurred rather abruptly at this time, and as a consequence a corresponding burst of decomposition gas was released. The pool level swelled, and melt was ejected above the sintered crust, visible through the dense aerosol.

Figure 7 shows an illustration of the debris configuration remaining after M1. The hatched region contains both the remnants of the original charge which formed the sintered bridge crust plus debris and particles atop the charge from the various eruption events. It was difficult to clearly distinguish these regions during dissection because the entire top region was "cemented" in sediment. The sediment had been left following water boiloff and consisted of released aerosol retained by the overlying water. About 20 kg of such sediment was collected based on preliminary estimate. No water nor sediment were found in the void crust and the solidified melt layer, indicating that no water penetrated the crust layer after the test. The bottom of the sintered crust had a layer of resolidified melt. Of particular note is that the melt had breached the crust along one wall and left an extruded mass exposed high up along the wall which solidified in place, depicted in Fig. 7. This suggests that the corium pool experienced volumetric swell with sufficient force that it was able to breach the overlying crust and extrude a large mass beyond the crust. Presently, it is not clear when this occurred. It is convenient to imagine that it may have occurred during the Event #1 ablation burst, in which case this mass would have contributed to the initial quench peak in Fig. 6. However, Event 1C is also a candidate since this event precipitated a large integrated heat removal which is otherwise difficult to explain.

SUMMARY OF FINDINGS

Both MACE tests M0 and M1 contributed important information to the MCCI and melt coolability data base although neither test fully met its objectives. Melt-water contact was achieved in M0, but after a period of intense energy removal a bridge crust formed which thereafter separated the water from the melt zone. Melt-water contact was not achieved in M1 owing to presence of a bridge crust as an initial condition. Key findings are summarized as follows:

1) The melt-water interaction stage of M0 was very vigorous, removed heat from the melt pool at 3.5 MW/m^2 for about three minutes, and extracted an amount of energy greater than the heat of solidification of the entire melt mass. There was no steam explosion.

2) M0 data suggests that basemat erosion was temporarily halted following the initial aggressive quench period.

3) A bridge crust was formed which anchored to the test section sidewalls and prevented water ingression into the corium zone. This would not be expected at reactor scale. The crust was sufficiently

porous to permit upward passage of concrete decomposition gasses.

4) Both tests M0 and M1 showed evidence of periodic occurrence of large pool swelling. The pool swelled to contact the underside of the crust and additionally caused extrusion of melt above the crust (eruption when accompanied by gas release/blowdown effects). This significantly augmented the corium quench process and depleted the remaining corium mass interacting with the concrete. The dispersed debris ranged from particles (which formed a particle bed atop the crust) to a large extruded mass. The pool void fraction increased to as high as 56% in M0 to account for this extrusion.

5) The upward heat flux after crust formation in M0 amounted to 600 kW/m^2 which gradually diminished to ~150 kW/m^2 as the extruded/dispersed mass grew in depth atop the crust.

6) Test M1 showed evidence of "ablation bursts" early in the test while appreciable metal remained in the corium composition.

7) Test M1 demonstrated the effectiveness of the overlying water to trap released aerosol.

It is premature to attempt to draw conclusions on melt coolability pertaining to the reactor system from the M0 and M1 tests. Their value lies first in guiding model development as regards the stages of cooling, crust formation, and pool swell effects. Secondly, these tests are stepping stones to improved tests addressing melt cooling phenomena.

ACKNOWLEDGEMENT

This work is performed under sponsorship of the Advanced Containment Experiments (ACE) international consortium organized by Electric Power Research Institute. The ERPI program manager is B. R. Seghal. The data is the property of the ACE Consortium, and the authors acknowledge their permission to release the information contained herein. The authors acknowledge the important contributions to the experiments by D. Bromberek, A. Kras, E. Pozzie, and J. Weber. The manuscript was prepared for publication by Ms. L. Ondracek.

REFERENCES

1. B. R. Seghal and B. W. Spencer, "ACE Program Phase C: Fission Product Release from Molten Corium-Concrete Interactions (MCCI)," submitted to OECD CSNI Specialist Meeting on Core Debris Concrete Interactions, Karlsruhe, Germany, April 1-3, 1992.

2. B. R. Seghal and B. W. Spencer, "ACE Program Phase D: Melt Attack and Coolability Experiment (MACE) Program," submitted to OECD CSNI Specialist Meeting on Core Debris Concrete Interactions, Karlsruhe, Germany, April 1-3, 1992.

3. J. J. Sienicki and B. W. Spencer, "The Jet Impingement Stage of Molten Core-Concrete Interactions," OECD CSNI Specialist Meeting on Core Debris/Concrete Interactions, Palo Alto, CA, September 3-5, 1986.

4. R. E. Blose, et. al., "Sustained Heated Metallic Melt/Concrete Interactions with Overlying Water Pools," NUREG/CR-4727, July 1987.

5. M. T. Farmer, et. al., "Modeling and Database for Melt-Water Interfacial Heat Transfer," submitted to OECD CSNI Specialist Meeting on Core Debris Concrete Interactions, Karlsruhe, Germany, April 1-3, 1992.

6. M. F. Roche, Argonne National Laboratory, private communication, November 1990.

7. M. L. Corradini and R. L. Engelstad, University of Wisconsin/Madison, private communication, January 1992.

Table 1. Specifications for MACE Test M1b

		M0	M1
Test Section Dimensions		30 x 30 cm	50 x 50 cm
Pressure, MPa absolute		0.1 (nominal)	0.1 (nominal)
Corium Mass, Kg		130	430
Collapsed Pool Depth, cm		15	25
Corium Type		PWR; Zr 70% oxidized	PWR; Zr 70% oxidized
Corium Composition at Onset of Ablation (Mass %)	UO_2	73 (56)	292 (68)
	ZrO_2	14 (11)	58 (13)
	Zr	5 (4)	19 (4)
	Fe	0	21 (5)
	SiO_2	4 (3)	0
	CaO	4 (3)	31 (7)
	Conc	30 (23)	10 (3)
Initial Melt Temperature, K		2000 (est)	2300 (est)
Specific Power, watts/kg UO_2 (actual)		350 (2x - 4x actual)	350 (1x - 2x actual)
Basemat Type		Limestone/Common Sand	Limestone/Common Sand
Basemat Height, cm		35	50
Ablation Depth at Water Addition, cm		1.2 cm	2.5 cm (8.0 cm actual)
Water Addition Rate, liter/second		10	2 (equivalent to 18 MW/m^2)
Water Collapsed Depth, cm		50	50
Water Makeup Rate, liter/second		10	2
Temperature of Added Water, K		296	296
DEH Power Operating Mode		Constant voltage	Constant voltage

Figure 1. Illustration of MACE Experiment Apparatus

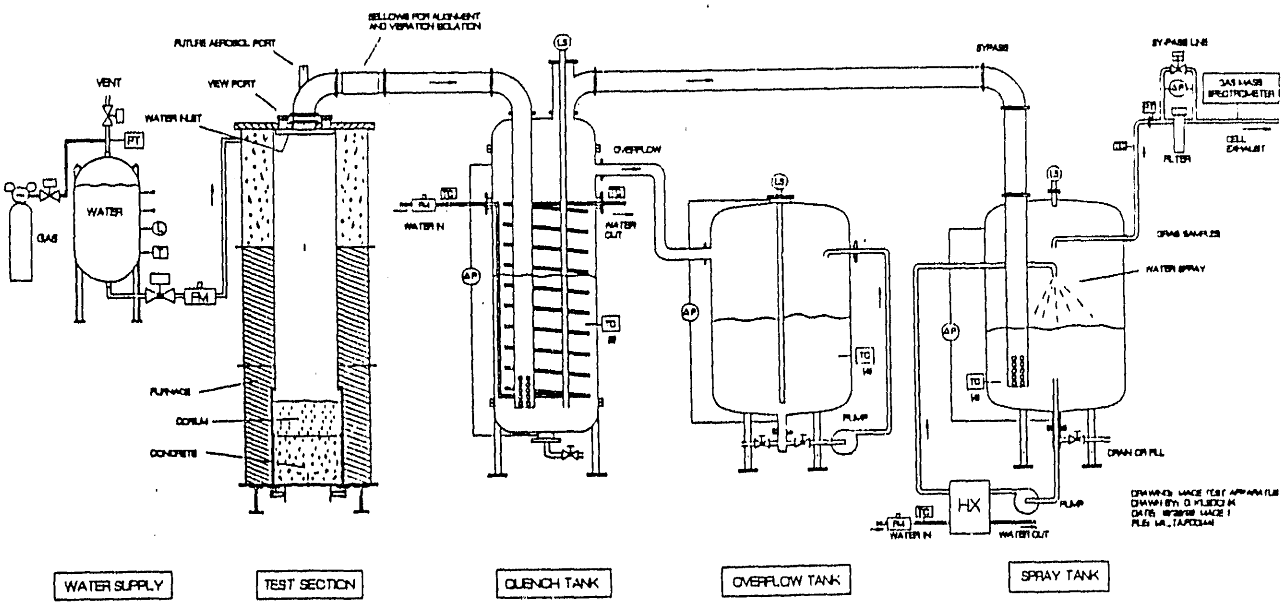

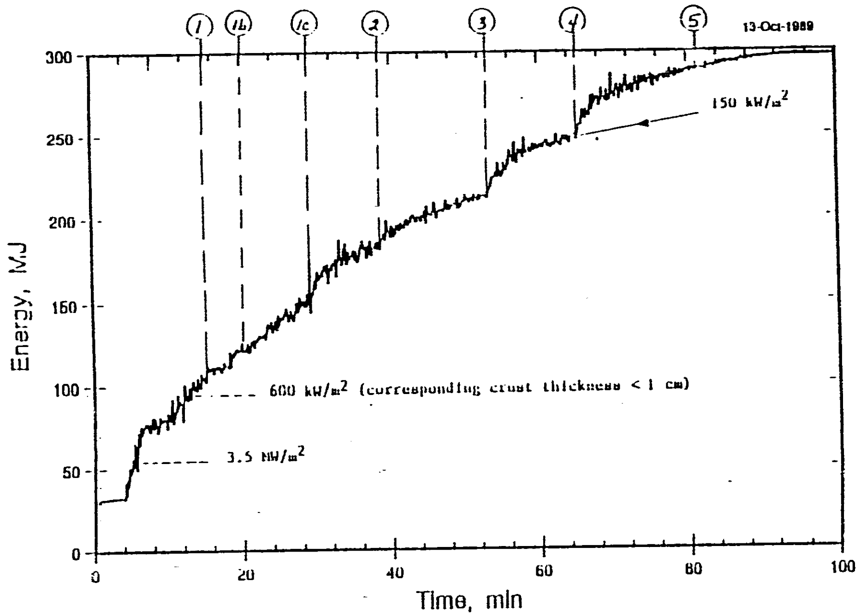

Figure 2. MO Upward Heat Removal from Melt Pool

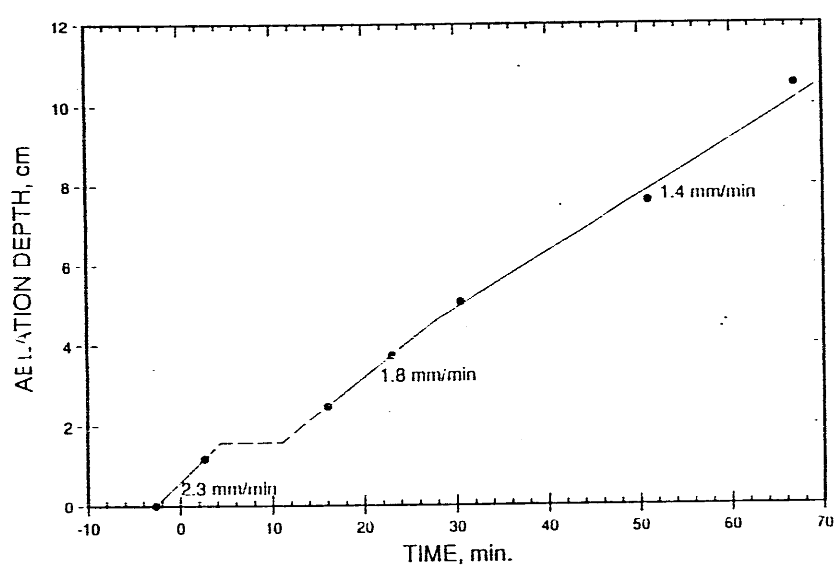

Figure 3. MO Centerline Ablation Data

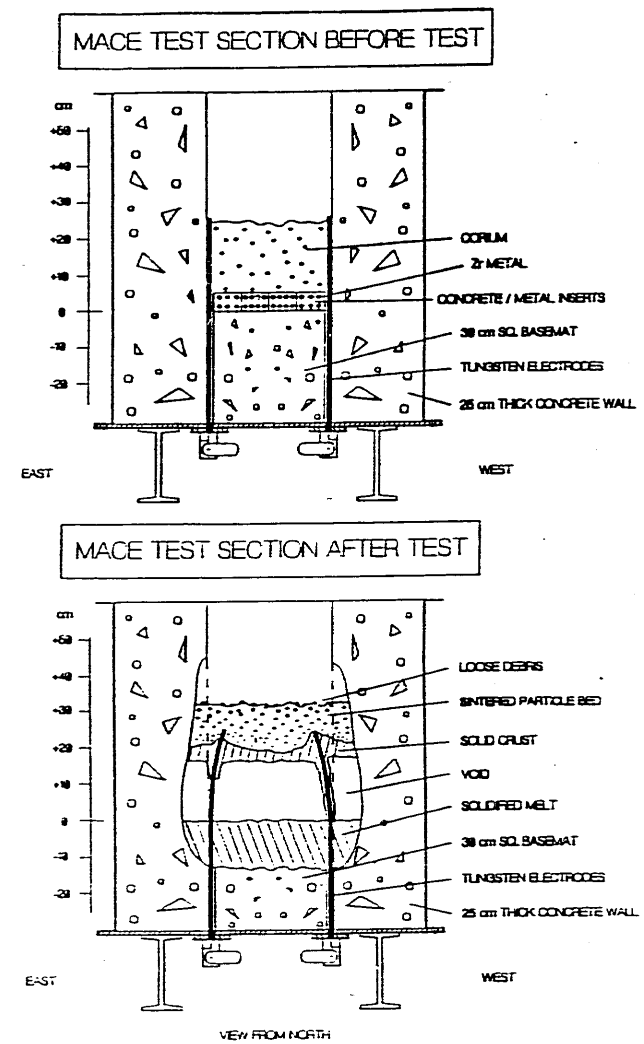

Figure 4. Illustration of MO Test Section

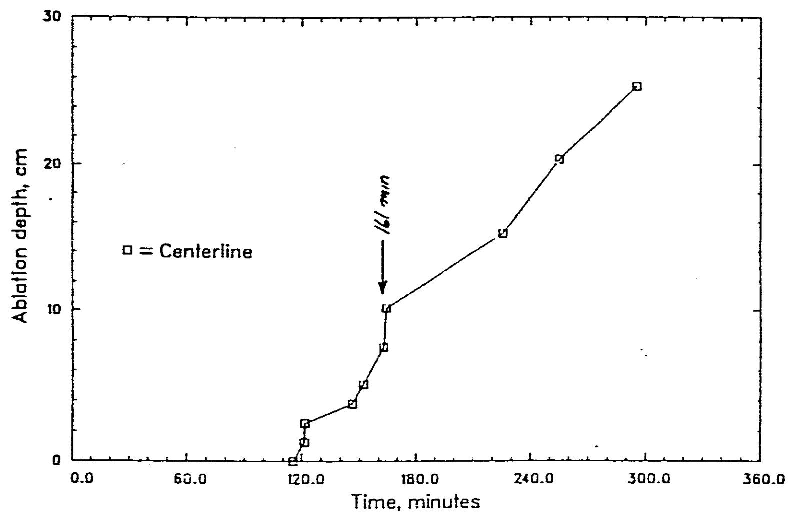

Figure 5. M1 Centerline Ablation Data

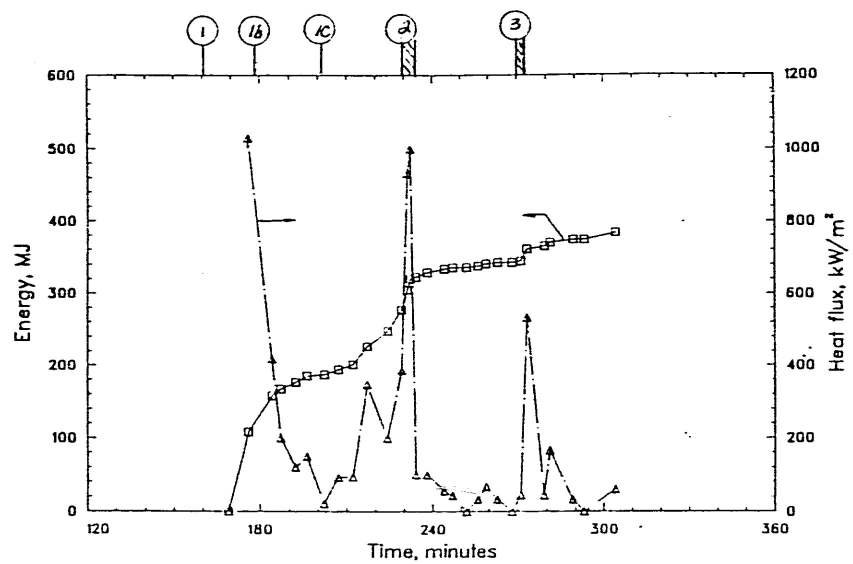

Figure 6. M1 Uncorrected Quench Rate Data

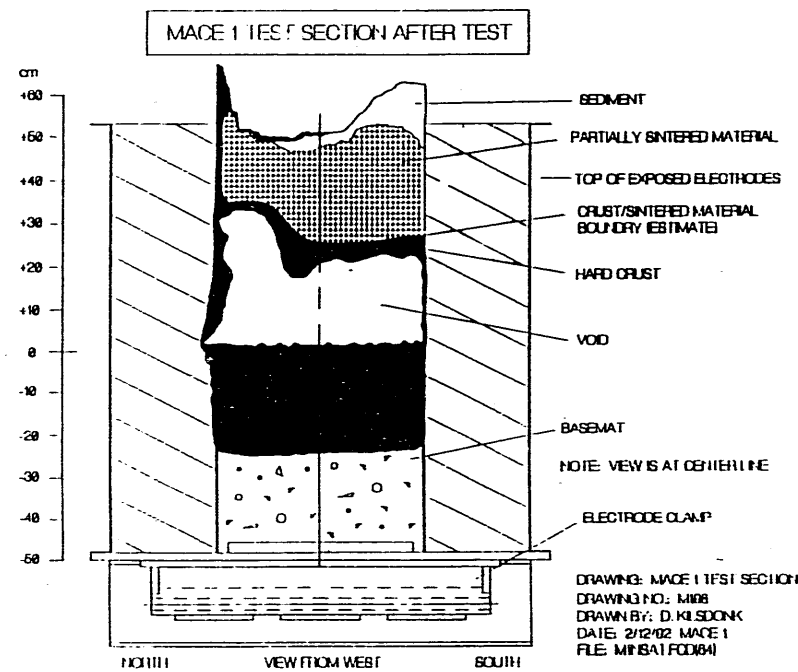

Figure 7. Illustration of M1 Posttest Debris Configuration

END

DATE FILMED

5/18/92